

Published in final edited form as:

Chem Res Toxicol. 2012 March 19; 25(3): 741–746. doi:10.1021/tx200540z.

Molecular basis of the mechanism of thiol oxidation by hydrogen peroxide in aqueous solution: challenging the S_N2 paradigm

Ari Zeida^a, Ryan Babbush^{a,b}, Mariano C. González Lebrero^c, Madia Trujillo^d, Rafael Radi^d, and Darío A. Estrin^a

^a Departamento de Química Inorgánica, Analítica y Química-Física and INQUIMAE-CONICET, Facultad de Ciencias Exactas y Naturales, Universidad de Buenos Aires, Ciudad Universitaria, Pab. 2, C1428EHA Buenos Aires, Argentina

^c IQUIFIB-Dpto. Química Biológica, Facultad de Farmacia y Bioquímica, Universidad de Buenos Aires, Buenos Aires, Argentina

^d Departamento de Bioquímica and Center for Free Radical and Biomedical Research, Facultad de Medicina, Universidad de la República, Av. Gral Flores 2125, CP 11800, Montevideo, Uruguay.

Abstract

The oxidation of cellular thiol containing compounds, such as glutathione and protein Cys residues, is considered to play an important role in many biological processes. Among possible oxidants, hydrogen peroxide (H_2O_2) is known to be produced in many cell types as a response to a variety of extracellular stimuli and could work as an intracellular messenger. This reaction has been reported to proceed through a S_N2 mechanism, but despite its importance, the reaction is not completely understood at the atomic level. In this work we elucidate the reaction mechanism of thiol oxidation by H_2O_2 for a model methanethiolate system using state of the art hybrid quantum-classical (QM-MM) molecular dynamics simulations. Our results show that the solvent plays a key role in positioning the reactants, that there is a significant charge redistribution in the first stages of the reaction, and that there is a hydrogen transfer process between H_2O_2 oxygen atoms that occurs after reaching the transition state. These observations contradict the S_N2 mechanism hypothesis for this reaction. Specifically, our results indicate that the reaction is driven by a tendency of the slightly charged peroxidatic oxygen to become even more negative in the product via an electrophilic attack on the negative sulfur atom. This is inconsistent with the S_N2 mechanism, which predicts a protonated sulfenic acid and hydroxyl anion as stable intermediates. These intermediates are not found. Instead, the reaction proceeds directly to unprotonated sulfenic acid and water.

Keywords

thiol containing compounds; hydrogen peroxide; oxidation; S_N2 ; redox signaling; redox regulation

^bPresent address: Department of Chemistry, Harvard University, 12 Oxford Street, Cambridge, MA, USA.

Supporting Information Available. Geometric parameters table, IRC calculations energetics table and figure, and 3D animation. This material is available free of charge via the Internet at <http://pubs.acs.org>

INTRODUCTION

Oxidation of cellular thiol containing compounds such as glutathione and protein Cys residues by reactive oxygen species, is considered to play important roles in a wide array of biological processes including signal transduction, regulation of the activity of enzymes, protein channels, transcription factors and antioxidant responses.¹⁻⁵ Hydrogen peroxide (H₂O₂) is produced in many cell types as a response to a variety of extracellular stimuli and could work as a ubiquitous intracellular messenger.⁶ Particularly, the two-electron oxidation of reactive protein Cys by H₂O₂ is a key event during redox signaling and regulation.⁷⁻⁹ Though this reaction has been productively studied, the exact mechanism remains poorly understood.

There is consensus about thiolates being much more prone to oxidation than protonated thiols¹⁰ and that they react with the protonated form of hydroperoxides.¹¹ The reduction of H₂O₂ by thiolates in aqueous solution has been described as a bimolecular nucleophilic substitution (S_N2) in which the thiolate acts as the nucleophilic moiety generating the breaking of the O–O peroxide bond and displacing the HO[−] leaving group.¹¹ However, recent theoretical studies have demonstrated that the product of the reaction would be H₂O instead of OH[−],¹²⁻¹⁵ which is inconsistent with a S_N2 mechanism. In this context, Chu and Trout have investigated the reaction between dimethylthiol and H₂O₂ via DFT calculations, analyzing the effect of the aqueous environment including up to three explicit water molecules.¹³ In successive works, using an IMOMO methodology, Cardey and Enescu modeled the oxidation of methanethiolate (CH₃S[−]) and Cys-thiolate (Cys-S[−]) by H₂O₂,^{14,15} including solvent effects through a Polarizable Continuum Model (PCM).

The overall oxidation reaction has been reported to occur through:



where RSO[−] is the deprotonated form of sulfenic acid. Oxidation rate constantsⁱ of the reaction on eq. 1 are in the ~10 M^{−1}s^{−1} range for low molecular weight thiols in aqueous solution.^{10,13,17} It has been found that rate constants exhibit almost no dependence on the thiol pK_a value and all considered low molecular weight thiols presented similar pH independent rate constants.¹⁰ The free energy barrier of the reaction of free Cys with H₂O₂ was estimated as 15.9 kcal/mol.¹⁸ Remarkably, the rate constants for peroxidatic thiols in Cys-dependent peroxidases are several order of magnitude larger, in the ~10⁴-10⁸ M^{−1}s^{−1} range.¹⁹⁻²¹ Moreover, very recent works proposed that protein environment could account for a hydrogen network and substrate placing such as to provide an alternative mechanism to the one found in aqueous solution.²²⁻²⁴ In this context, a S_N2 or other kind of mechanism may explain the higher reaction rates in enzyme-catalyzed reductions of hydrogen peroxide.²⁵

Clearly the reaction mechanism of this extremely relevant reaction is not still understood from a molecular viewpoint. As a first step towards elucidating this mechanism we present an integrated QM-MM investigation of the oxidation of methanethiolate (CH₃S[−]) by H₂O₂, embedded in a classical water molecules box, under periodic boundary conditions. The choice of methanethiolate is due to its small size which allows for more efficient sampling in the expensive QM-MM MD simulations. This is justified by the fact that for low molecular weight thiols the reported rate constants of oxidation by H₂O₂ are very similar, suggesting

ⁱWe refer to real, pH independent rate constants which are related to apparent, pH dependent rate constants through the fractions of available thiolate and of available protonated peroxide at a given pH, as follow:

that the same mechanism is operative.¹⁰ Our model is a realistic representation of the aqueous environment at room temperature.

We explore the reaction by means of QM-MM MD simulations using an umbrella sampling scheme.²⁶ This approach allowed us to obtain thermodynamical information such as the free energy profile in

$$k_{\text{pH dependent}} = k_{\text{pH independent}} \times \frac{K_{a_{\text{RSH}}}}{K_{a_{\text{RSH}}} + [\text{H}^+]} \times \frac{[\text{H}^+]}{K_{a_{\text{H}_2\text{O}_2}} + [\text{H}^+]}$$

Where $K_{a_{\text{RSH}}}$ is the acidity constant of the thiol and $K_{a_{\text{H}_2\text{O}_2}}$ is the acidity constant of H_2O_2 , which has a pK_a value of ~ 11.7 ,¹⁶ and therefore is fully protonated at near physiological pHs. addition to microscopic insight about electronic structure changes throughout the reaction. The results presented in this work suggest that the process cannot be considered as a simple substitution since the product formation involves a hydrogen atom transfer.

The data reported herein provides a detailed microscopic view of the thiolate oxidation reaction by H_2O_2 in water, and is the first step for future studies related to the mechanisms of thiolate oxidation in different protein environments.

METHODS

Initial Survey of the System in Vacuum and Implicit Solvent

In order to obtain valid starting structures for further analysis, to obtain information about the energy surface and the mechanism of the reaction under investigation, and to carry out a methodology evaluation, we performed several electronic structure calculations using *Gaussian 03*.²⁷ The structures of reactants complex (RC) ($\text{H}_2\text{O}_2/\text{CH}_3\text{S}^-$), products complex (PC) ($\text{H}_2\text{O}/\text{CH}_3\text{SO}^-$) and transition state (TS) were optimized both *in vacuo* and in aqueous solution via the PCM approach,²⁸ at different levels of theory: *HF*, *PBE*, *B3LYP*, *MP2*, employing a double-zeta plus polarization (*dzvp*) *Gaussian* basis set.²⁹ Frequency calculations were performed in all cases. Aiming to investigate if one or more water molecules could be involved in the reaction mechanism, we also performed IRC calculations at the *PBE/dzvp* level of theory including one and four water molecules in the QM system, both *in vacuo* and with the PCM method.

The geometry of RC obtained with the *B3LYP* functional was used as the starting point for a first approximation of the energy profile using the PCM solvation model, in which the reaction coordinate was taken to be the distance between the sulfur atom (S) and the reactive oxygen in the peroxide (O_r) in order to obtain partial charges necessary to perform the classical MD simulations which are required to equilibrate the systems, as described below.

QM-MM molecular dynamics simulations

The actual QM-MM simulations were carried out using our own developed program (for details on the QM-MM scheme see refs.^{30,31}). The solute was embedded in a 24 Å cubic box, containing 490 explicit water molecules simulated using the TIP4P mean-field potential.³² The constraints associated with the intermolecular distances in the solvent were treated using the SHAKE algorithm.³³ The Lennard-Jones parameters (ϵ and σ) for the quantum subsystem atoms were 0.250, 0.172, 0.170 and 0.016 kcal/mol, and 3.563, 3.399, 3.250 and 1.069 Å, for S, O, C and H, respectively. For the QM region (CH_3S^- and H_2O_2 atoms), computations were performed at the generalized gradient approximation (GGA) level, using the *PBE* combination of exchange and correlation functionals, with a *dzvp* basis

set for the expansion of the one-electron orbitals. The electronic density was also expanded in an auxiliary basis set and the coefficients for the fitting were computed by minimizing the error in the Coulomb repulsion energy.²⁹

All the QM-MM MD simulations were run for at least 4 ps and employed the Verlet algorithm to integrate Newton's equations with a time step of 0.2 fs. Initial configurations were generated from preliminary 100 ps classical equilibration runs in which the solute was treated classically as a rigid moiety with the RESP charges described above. At $t=0$, the classical solute was replaced by a solute described at the DFT level, according to the methodology described above. An additional 2 ps of equilibration was performed using the QM-MM scheme. During the simulations, the temperature was held constant at 300 K using the Berendsen thermostat.³³ The solute and the rest of the system were coupled separately to the temperature bath.

We employed an umbrella sampling scheme, choosing as reaction coordinate the difference between the O_r-O_w and the $S-O_r$ distances, which was sampled from -1.5 to 1.5 Å. The harmonic potentials used had spring constants of about 3000 N/m. 31 simulation windows were employed to obtain the free energy profiles.

All dynamics visualizations and molecular drawings, were performed with *VMD 1.8.6*.³⁴

RESULTS AND DISCUSSION

The free energy profile

After *Gaussian* geometry optimizations and first initial survey of the system, we performed molecular dynamics simulations using the QM-MM scheme as described above. The obtained free energy profile is depicted in Figure 1.

The free energy profile obtained in aqueous solution shows a free energy barrier of ~18 kcal/mol, which is in good agreement with previous experimental¹⁸ and theoretical¹³⁻¹⁵ data available for low molecular weight thiol oxidations by hydrogen peroxide. As expected, the reaction is clearly exergonic, with a change in free reaction energy of about -52 kcal/mol, also in agreement with previously reported information.¹⁴

In order to get an estimation of the reliability of DFT in predicting the energetics, we performed characterizations of RC, TS, PC, using different methods (*HF*, *PBE*, *B3LYP* and *MP2*), both *in vacuo* and in aqueous solution via the PCM approach, with a *dzvp* basis set (Table 1 summarizes the results). Frequencies calculations were carried out in all cases.

It is worth noticing that all structures optimized in this section are very comparable within the different methodologies applied (see Supplementary Information Table 1). As expected, the use of *PBE* leads to underestimation of barriers in comparison with those obtained with *B3LYP* or *MP2*.³⁵

We found that the inclusion of the environment by means of PCM has a significant effect within all models tested here, lowering about 20% the computed values. Furthermore, for all the calculations including the environment effect, except for *HF* calculations (overestimated barriers), activation barriers are in the range of experimental reports for this kind of reactions.¹⁸

However, this apparent qualitative agreement in the computed energetics may be misleading, because both the isolated species and the PCM solvated species exhibit geometrical features in the RC structure that are completely unrealistic for describing the actual situation in aqueous solution. Specifically, the inspection of the geometries reached

with both strategies show that, while the vacuum and PCM structures of TS and PC are qualitatively similar to those sampled in the QM-MM simulations, the RC adopts significantly different conformations when explicit waters are present (see Supplementary Information Table 1). With little differences, every geometry optimization performed for the isolated and PCM solvated RC, resulted in a “symmetric” conformation, where the distances between the S atom and both O atoms of the peroxide are practically the same; the same fact is observed for the distances between the S atoms and the H atoms of the peroxide, resulting in a *cis*-H₂O₂ (Figure 2a). In contrast, the average conformation of the RC sampled by our QM-MM scheme is an “asymmetric” one, where the O_r atom is much closer to the S atom than O_w, and the peroxide adopts a *trans* configuration (Figure 2b). Consistent with the work described by Chu *et al.*,¹³ in the presence of 2-3 explicit water molecules, specific solute-water interactions can form favoring the “asymmetric” arrangement. Since neither *in vacuo* nor implicit solvents environments allowed these specific interactions, the “symmetric” conformation in which solute atom contacts are maximized is the result of such calculations. Consequently, the RC energies achieved with these two different approaches are not comparable.

In order to explore the possibility of water molecules being involved in the reaction mechanism, we performed IRC calculations including 1, and 4 water molecules, in the QM system, both *in vacuo* and with the PCM model. The presence of waters molecules modifies the geometry of the RC in a similar way of that observed in the QM-MM simulation. However, as reported by Chu *et al.* in a similar model system,¹³ no significant differences in the reaction mechanism and energetics are observed by including water molecules (see Table S2 and Figure S1 of Supporting Information).

Reaction evolution

Three major events occur during the reaction: the breaking of O–O bond of the peroxide, the formation of the bond between the sulfur (S) and the reactive oxygen (O_r) and the transfer of the hydrogen (H_i) bound to O_r to the other oxygen of H₂O₂ (O_w). Our QM-MM scheme allows us to get a microscopic insight into the reaction evolution and mechanism (see the 3D animation available in Supporting Information for illustration).

A close examination of the early TS structure reveals an alignment between S, O_r and O_w (see Supplementary Information Table 1). Additionally, H_i is still attached to O_r, as shown in the distance versus reaction coordinate plot (Figure 3). This analysis also indicates that the transfer of H_i takes place “downhill”, barrierless, after the system has reached the TS. Therefore, even though the product sulfenic acid appears in its unprotonated form, from a kinetic point of view the leaving group of the reaction could be considered as a hydroxyl, which is in agreement with reaction rates correlation with the conjugated acid of the leaving group pK_a.³⁶

The dependence of the Mulliken population over different moieties upon reaction is shown in Figure 4. The system negative charge is in the RC, localized mostly in the S atom, while oxygen atoms of H₂O₂ possess negative charges of roughly -0.5 e each. Based on experimental results which indicate that all low molecular weight thiols exhibit similar pH independent oxidation rate constants, it has been suggested that charge transfer is not significantly involved in the formation of the transition state.¹⁹ However, our results indicate a significant charge rearrangement during the first steps of the reaction resulting in negative charge from the RC distributed across both peroxide O atoms and the S atom. This does not contradict experimental rate constants, since decreases in the solvation in the TS (see below) can cause a significant decrease in the observed dependence of the rate on the basicity of the nucleophile.³⁷ Although in the PC, both O_r and O_w atoms possess a charge of about -1 e as would be the case in a homolytic rupture, the reorganization of oxygen charges is not

entirely symmetric. O_w suffers a faster decrease (reaching a final status consistent with a water oxygen atom charge) while O_r does not reach its final charge until it is bonded with S, acquiring most of the negative charge of the CH_3SO^- moiety. The methyl group preserves its close to zero charge along the entire process.

Solvation

Previous studies have modeled solvation effects in this kind of reaction using either continuum models or the inclusion of a small number of explicit water molecules by means of geometry optimizations.^{13-15,38} Our QM-MM MD approach allows us to obtain a more realistic picture of solvation in bulk water at room temperature. We have analyzed the solvation structure along the process, to monitor how solvation patterns may affect the reaction energetics. Radial correlation functions of selected atoms with water oxygen atoms from the RC (left panel), TS (middle panel) and PC (right panel), along with representative snapshots of each step, are shown in Figure 5.

Radial correlation functions of S atom show that this moiety loses its hydrophilicity along the reaction. The opposite effect is observed in both oxygen atoms. While in the RC the oxygens are poorly solvated, they become better solvated in the TS due to the early charges redistribution and strongly solvated in the PC. Moreover, the peaks of both peroxide oxygen atoms observed in the TS and PC are located at ~ 2.8 Å (radial distance), while the S peak in the RC is ~ 3.2 Å, confirming that it is much more favorable to solvate O^- like atoms than the S^- one. These observable facts lead to a PC much better solvated than the RC and the TS.

CONCLUSIONS

We present here an integrated QM-MM approach for the oxidation of CH_3S^- by H_2O_2 , which allow us to get microscopic dynamical information of this reaction in aqueous environment. The energetics obtained are in good agreement with previous experimental¹⁸ and theoretical¹³⁻¹⁵ reported data and also with quantum calculations presented herein.

We found that the transfer of the hydrogen atom from the reactive peroxidatic oxygen to the non-reactive one takes place after reaching the TS and without an energy barrier; thus, a water molecule appears in the products, suggesting that in aqueous solution the protonated form of the product sulfenic acid is never produced. Although the calculations performed in this work suggests that no water molecules are chemically involved in the process, the solvent plays an important role in the reaction, particularly in the reactants structure. Furthermore, the activation energy is due to two main events: the alignment of the sulfur atom with the peroxidatic oxygen atoms and a significant charge redistribution, which correlates with important changes in the solvation profile. This phenomenon emphasizes the key role of the environment in modulating thiol reactivity, which can be explicitly evaluated by our QM-MM scheme.

In summary, our microscopic insight is not in agreement with the S_N2 paradigm because the product formation involves a hydrogen atom transfer which precludes the possibility of a simple substitution. Even though the initial attack of the reactant thiolate to an oxygen atom of H_2O_2 is an attack between two negative charged centers, the peroxidatic oxygen electrophilicity is the true driving force in this process as evidenced by significant electron donation from the thiolate to the peroxide in the TS.

Thiol groups in cysteine containing proteins usually react with peroxides with similar rate constants as low-molecular weight thiols.³⁹ However, there are some highly reactive thiols which reduce peroxides surprisingly fast. This is the case for the reaction of hydrogen

peroxide reduction by thiol-dependent peroxidases such as peroxiredoxins. Fast reactivity was initially considered to be related to the low peroxidatic thiol pK_a that assured thiolate availability at physiological pHs. However, it is now widely recognized that increased thiolate availability cannot explain differences in reactivities by factors of $\sim 10^6$ - 10^7 as have been reported for H_2O_2 reduction by peroxidatic thiols in some peroxiredoxins compared with the uncatalyzed reaction. Very recently, active site microenvironmental factors leading to transition state stabilization have been considered.^{9,19,23} The results presented here emphasize the importance for the protein environment that surrounds these thiols, to contribute in the alignment of the S atom with the peroxide O atoms in the TS,^{23,40,41} so that a substantial charge reorganization can take place. Moreover, differences involving aqueous and specialized protein environments could produce major changes in the reaction mechanism, perturbing the energetics of PC, TS and RC, and/or modifying the reactants electrophilicity. For example, in the case of peroxiredoxins it has been proposed that the presence of nearby residues such as arginine, proline and threonine, may form an active hydrogen network that could assist in placing the substrate and making a simple substitution mechanism possible.²³ Information about the atomistic detailed mechanism of thiol containing compounds oxidation with other oxidants such as peroxynitrite is still scarce. In this context, experimental and theoretical studies are underway in our laboratories, to shed light on the mechanisms of thiol oxidation and the broad modulation of thiol reactivity in proteins towards oxidants and electrophiles.

Supplementary Material

Refer to Web version on PubMed Central for supplementary material.

Acknowledgments

Funding Support.

This work was partially supported by the University of Buenos Aires, CONICET and Centro de Biología Estructural Mercosur (CEBEM). A portion of the funding for this work was made possibly by a United States NSF REU grant. The calculations have been performed in FCEN CECAR and MINCYT Cristina computer centers. R.R. and M.T. acknowledge the financial support of the Howard Hughes Medical Institute, National Institutes of Health, Agencia Nacional de Investigación e Innovación (ANII, Uruguay) and Comisión Sectorial de Investigación Científica (CSIC), Universidad de la República.

ABBREVIATIONS

DFT	density functional theory
IMOMO	integrated molecular orbital + molecular orbital
MD	molecular dynamics
dzvp	double zeta valence with polarization
IRC	intrinsic reaction coordinate
RESP	restrained electrostatic potential

REFERENCES

1. Poole LB, Nelson KJ. Discovering mechanisms of signaling-mediated cysteine oxidation. *Curr. Opin. Chem. Biol.* 2008; 12:18–24. [PubMed: 18282483]
2. Bindoli A, Fukuto JM, Forman HJ. Thiol chemistry in peroxidase catalysis and redox signaling. *Antioxid. Redox Signal.* 2008; 10:1549–1564. [PubMed: 18479206]

3. Poole LB, Karplus PA, Claiborne A. Protein sulfenic acids in redox signalling. *Annu. Rev. Pharmacol. Toxicol.* 2004; 44:325–347. [PubMed: 14744249]
4. Claiborne A, Yeh JI, Mallett TC, Luba J, Crane EJ, Parsonage D. Protein-sulfenic acids: diverse roles for an unlikely player in enzyme catalysis and redox regulation. *Biochem.* 1999; 38:15407–15416. [PubMed: 10569923]
5. Barford D. The role of cysteine residues as redox-sensitive regulatory switches. *Curr. Opin. Struct. Biol.* 2004; 14:679–686. [PubMed: 15582391]
6. Rhee SG, Kang SW, Jeong W, Chang TS, Yang KS, Woo HA. Intracellular messenger function of hydrogen peroxide and its regulation by peroxiredoxins. *Curr. Opin. Cell Biol.* 2005; 17:183–189. [PubMed: 15780595]
7. Jones DP. Radical-free biology of oxidative stress. *Am. J. Physiol. Cell Physiol.* 2008; 295:849–868.
8. Stone JR, Yang S. Hydrogen peroxide: a signaling messenger. *Antioxid. Redox Signal.* 2006; 8:243–270. [PubMed: 16677071]
9. Winterbourn CC, Hampton MB. Thiol chemistry and specificity in redox signalling. *Free Radic. Biol. Med.* 2008; 45:549–561. [PubMed: 18544350]
10. Winterbourn CC, Metodiewa D. Reactivity of biologically important thiol compounds with superoxide and hydrogen peroxide. *Free Radic. Biol. Med.* 1999; 27:322–328. [PubMed: 10468205]
11. Edwards, JO. In *Peroxide Reaction Mechanisms*. Edwards, JO., editor. Interscience; New York: 1962. p. 67-106.
12. Bach RD, Su M, Schlegel BH. Oxidation of amines and sulfides with hydrogen peroxide and alkyl hydrogen peroxide. The nature of the oxygen-transfer step. *J. Am. Chem. Soc.* 1994; 116:5379–5391.
13. Chu JW, Trout BL. On the mechanisms of oxidation of organic sulfides by H₂O₂ in aqueous solutions. *J. Am. Chem. Soc.* 2004; 126:900–908. [PubMed: 14733566]
14. Cardey B, Enescu M. A computational study of thiolate and selenolate oxidation by hydrogen peroxide. *Chemphyschem.* 2005; 6:1175–1180. [PubMed: 15883994]
15. Cardey B, Enescu M. Selenocysteine versus cysteine reactivity: A theoretical study of their oxidation by hydrogen peroxide. *J. Phys. Chem. A.* 2007; 111:673–678. [PubMed: 17249758]
16. Evans MG, Uri N. The dissociation constant of hydrogen peroxide and the electron affinity of the HO₂ radical. *Trans. Faraday Soc.* 1949; 45:224–230.
17. Feliers C, Patria L, Morvan J, Laplanche A. Kinetics of oxidation of odorous sulfur compounds in aqueous alkaline solution with H₂O₂. *Env. Technol.* 2001; 22:1137–1146. [PubMed: 11766036]
18. Luo D, Smith SW, Anderson BD. Kinetics and mechanism of the reaction of cysteine and hydrogen peroxide in aqueous solution. *J. Pharm. Sci.* 2005; 94:304–316. [PubMed: 15570599]
19. Parsonage D, Youngblood DS, Sarma GN, Wood ZA, Karplus PA, Poole LB. Analysis of the link between enzymatic activity and oligomeric state in AhpC, a bacterial peroxiredoxin. *Biochem.* 2005; 44:10583–10592. [PubMed: 16060667]
20. Manta B, Hugo M, Ortiz C, Ferrer-Sueta G, Trujillo M, Denicola A. The peroxidase and peroxynitrite reductase activity of human erythrocyte peroxiredoxin 2. *Arch. Biochem. Biophys.* 2009; 484:146–154. [PubMed: 19061854]
21. Navrot N, Collin V, Gualberto J, Gelhaye E, Hirasawa M, Rey P, Knaff DB, Issakidis E, Jacquot JP, Rouhier N. Plant glutathione peroxidases are functional peroxiredoxins distributed in several subcellular compartments and regulated during biotic and abiotic stresses. *Plant Physiol.* 2006; 142:1364–1379. [PubMed: 17071643]
22. Ferrer-sueta G, Manta B, Botti H, Radi R, Trujillo M, Denicola A. Factors affecting protein thiol reactivity and specificity in peroxide reduction. *Chem. Res. Toxicol.* 2011; 24:434–450. [PubMed: 21391663]
23. Hall A, Parsonage D, Poole LB, Karplus PA. Structural evidence that peroxiredoxin catalytic power is based on transition-state stabilization. *J. Mol. Biol.* 2010; 402:194–209. [PubMed: 20643143]

24. Nagy P, Kerton A, Betz A, Peskin AV, Pace P, O'Reilly RJ, Hampton MB, Radom L, Winterbourn CC. Model for the exceptional reactivity of peroxiredoxins 2 and 3 with hydrogen peroxide; a kinetic and computational study. *J. Biol. Chem.* 2011; 286:18048–18055. [PubMed: 21385867]
25. Roos G, Messens J. Protein sulfenic acid formation: from cellular damage to redox regulation. *Free Radic. Biol. Med.* 2011; 51:314–326. [PubMed: 21605662]
26. Kumar S, Rosenberg JM, Bouzida D, Swendsen RH, Kollman PA. The weighted histogram analysis method for free energy calculations on biomolecules. I. The method. *J. Comp. Chem.* 1992; 13:1011–1021.
27. Gaussian 03. Gaussian, Inc.; Wallingford CT: 2004.
28. Tomasi J, Mennucci B, Cammi R. Quantum mechanical continuum solvation models. *Chem. Rev.* 2005; 105:2999–3093. [PubMed: 16092826]
29. Godbout N, Salahub DR, Andzelm J, Wimmer E. Optimization of Gaussian-type basis sets for local spin density functional calculations. Part I. Boron through neon, optimization technique and validation. *Can. J. Chem.* 1992; 70:560–571.
30. González Lebrero MC, Bikiel DE, Elola MD, Estrin DA, Roitberg AE. Solvent-induced symmetry breaking of nitrate ion in aqueous clusters: A quantum-classical simulation study. *J. Chem. Phys.* 2002; 117:2718–2725.
31. González Lebrero MC, Estrin DA. QM-MM investigation of the reaction of peroxynitrite with carbon dioxide in water. *J. Chem. Theo. Comp.* 2007; 3:1405–1411.
32. Jorgensen WL, Chandrasekhar J, Madura J, Impey RW, Klein M. Comparison of simple potential functions for simulating liquid water. *J. Chem. Phys.* 1983; 79:926–935.
33. Berendsen HJC, Postma JPM, Gunsteren WF, Van, DiNola A, Haak JR. Molecular dynamics with coupling to an external bath. *J. Chem. Phys.* 1984; 81:3684–3690.
34. Humphrey W, Dalke A, Schulten K. VMD: visual molecular dynamics. *J. Molec. Graphics.* 1996; 14:33–38.
35. Zhao Y, Truhlar DG. Density functionals with broad applicability in chemistry. *Acc. Chem. Res.* 2008; 41:157–167. [PubMed: 18186612]
36. Trindade DF, Cerchiaro G, Augusto O. A role for peroxymonocarbonate in the stimulation of biothiol peroxidation by the bicarbonate/carbon dioxide pair. *Chem. Res. Toxicol.* 2006; 19:1475–1482. [PubMed: 17112235]
37. Jencks WP, Haber MT, Herschlag D, Nazaretian KL. Decreasing reactivity with increasing nucleophile basicity. The effect of solvation on β_{nuc} for phosphoryl transfer to amines. *J. Am. Chem. Soc.* 1986; 108:479–483. [PubMed: 22175464]
38. Bayse C. Transition states for cysteine redox processes modeled by DFT and solvent-assisted proton exchange. *Org. Biomol. Chem.* 2011; 9:4748–4751. 2011. [PubMed: 21597638]
39. Trujillo, M.; Alvarez, B.; Souza, JM.; Romero, N.; Castro, L.; Thomson, L.; Radi, R. Mechanisms and biological consequences of peroxynitrite-dependent protein oxidation and nitration.. In: Ignarro, LJ., editor. *Nitric Oxide: Biology and Pathobiology*. Elsevier; Los Angeles: 2010. p. 61-102.
40. Karplus, PA.; Hall, A. Structural survey of the peroxiredoxins: structures and functions.. In: Flohe, L.; Harris, JR., editors. *Peroxiredoxins Systems*. Springer; New York: 2007. p. 41-60.
41. Hall A, Nelson K, Poole LB, Karplus PA. Structure-based insights into the catalytic power and conformational dexterity of peroxiredoxins. *Antioxid. Redox Signal.* 2011; 15:795–815. 2011. [PubMed: 20969484]

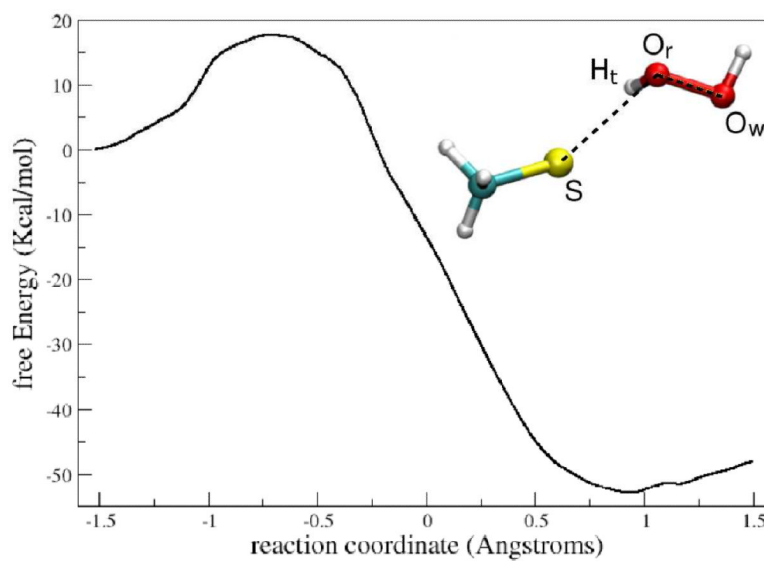


Figure 1.

Free energy profile obtained by umbrella sampling. Free energy (kcal/mol) is plotted versus reaction coordinate (Å). An illustrative picture with the reaction coordinate distance components and atom names as referred in the text is also shown.

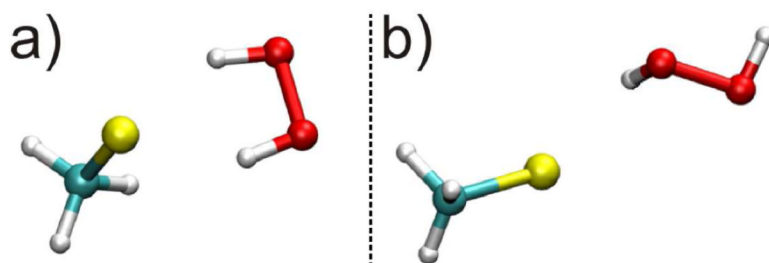


Figure 2.

RC conformations comparison. a) PBE/dzvp/PCM geometry of the RC. Note that both peroxide O atoms and their respective H atoms are in a quasi equidistant position from the S atom, in a “symmetric” conformation. b) average structure of the RC sampled with our QM-MM scheme. Oxygen atoms from the peroxide are not equidistant from the S atom, the angle between S-Or-Ow is $\sim 50^\circ$ larger than the angle obtained through in vacuo and PCM optimizations and the H_2O_2 shows a *trans* configuration.

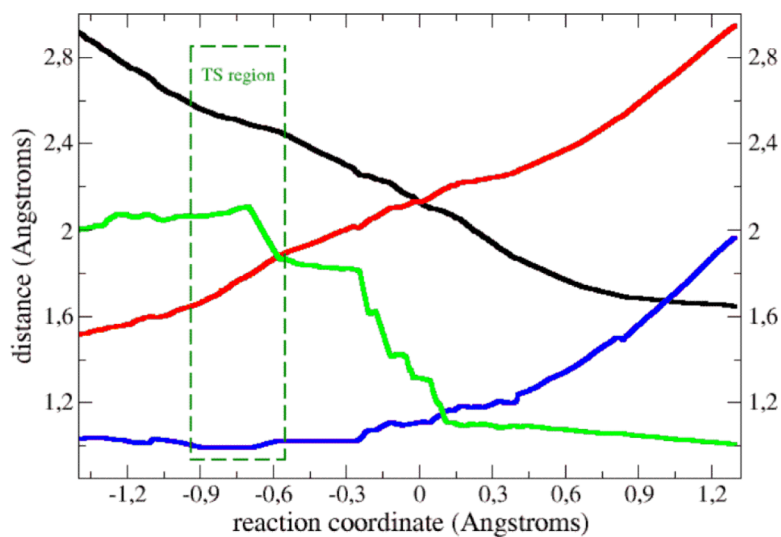


Figure 3. Bond length evolution during the reaction. The distances S-O_r, O_r-O_w, O_r-H_t, O_w-H_t (Å) as a function of the reaction coordinate are depicted using black, red, blue, and light green lines, respectively. The TS region (as determined in Figure 1) is indicated by a dark green box.

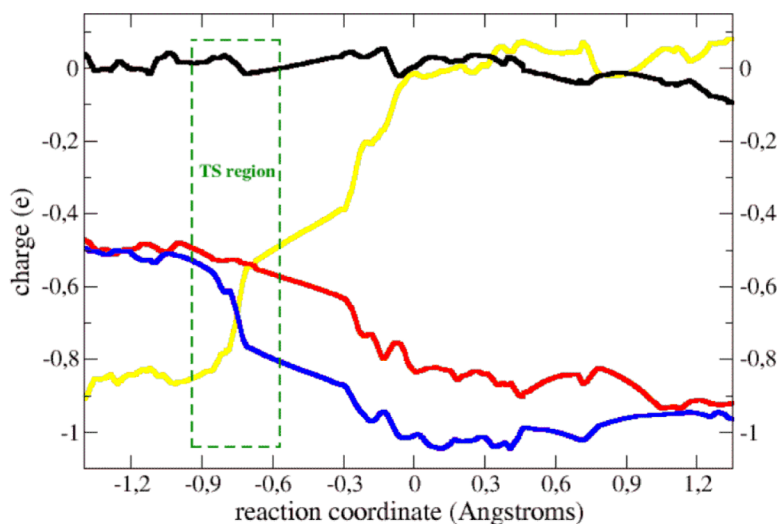


Figure 4.

Charge evolution during the reaction. Mulliken charges (e) of S atom (yellow line), O_r atom (red line), O_w atom (blue line) and methyl group (black line) are plotted versus the reaction coordinate (\AA). The TS region (as determined in Figure 1) is indicated by a dark green box.

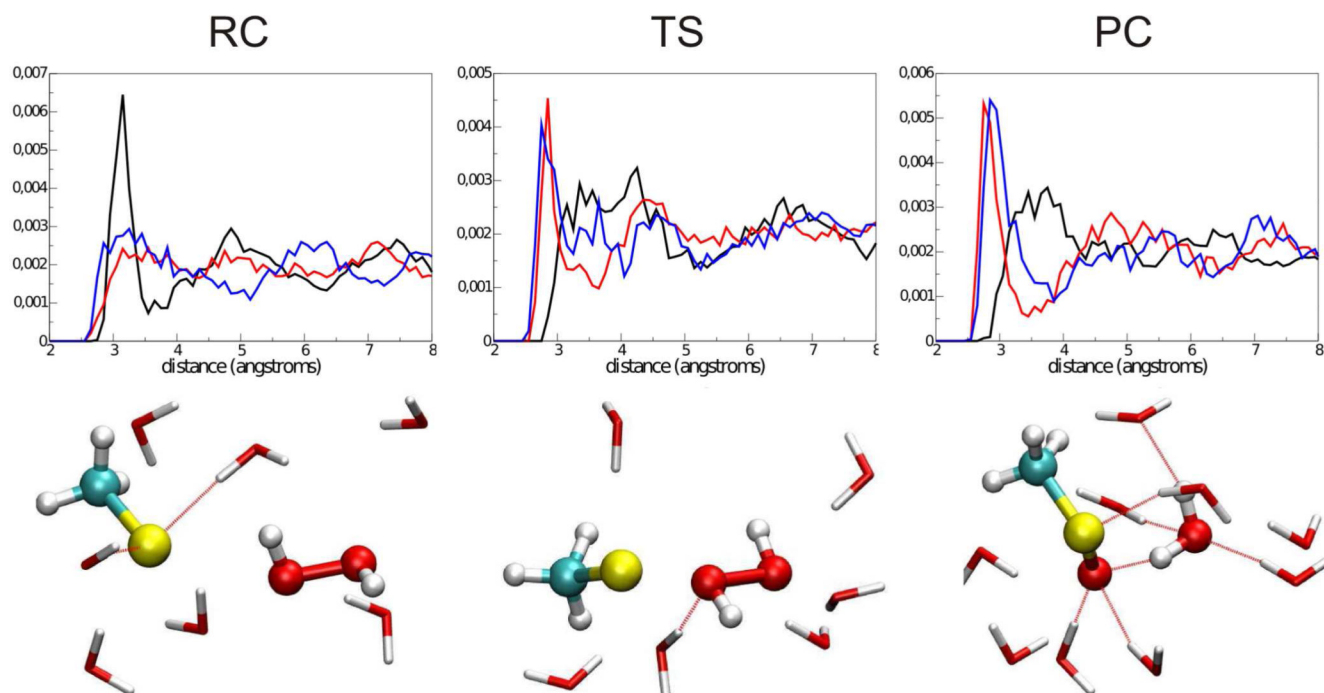


Figure 5. Solvation structure. Up: radial correlations functions of S (black line), O_r (red line) and O_w (blue line) with water oxygen atoms from the RC (left panel), TS (middle panel) and PC (right panel). Down: representative snapshots of the solvation structure of the RC (left panel), TS (middle panel) and PC (right panel).

TABLE 1

Reaction Energetics (kcal/mol) for isolated and PCM solvated species

Method	E_{act}	ΔG_{act}	E_{react}	ΔG_{react}
<i>HF/dzvp (in vacuo)</i>	50.2	50.1	-37.1	-36.1
<i>HF/dzvp (PCM)</i>	43.8	41.9	-43.8	-44.2
<i>PBE/dzvp (in vacuo)</i>	15.1	13.9	-33.1	-32.5
<i>PBE/dzvp (PCM)</i>	10.5	8.4	-39.0	-39.7
<i>B3LYP/dzvp (in vacuo)</i>	19.8	18.0	-35.3	-35.3
<i>B3LYP/dzvp (PCM)</i>	15.1	13.3	-42.3	-38.7
<i>MP2/dzvp (in vacuo)</i>	22.7	21.0	-43.1	-43.1
<i>MP2/dzvp (PCM)</i>	14.7	14.8	-52.0	-51.8